

PAPER • OPEN ACCESS

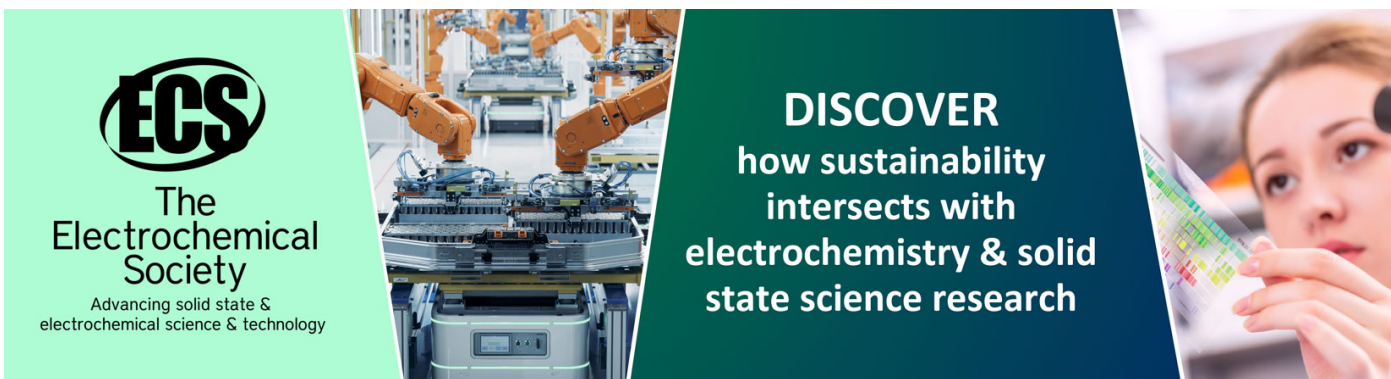
Simulation of ejector for vacuum generation

To cite this article: L Macia *et al* 2019 *IOP Conf. Ser.: Mater. Sci. Eng.* **659** 012002

View the [article online](#) for updates and enhancements.

You may also like

- [Thermodynamic Analysis of Two-Phase Ejector as Expansion Device with Dual Evaporator Temperatures on Split Type Air Conditioning Systems](#)
M E Arsana, I G B Wijaya Kusuma, M Sucipta et al.
- [Simultaneous measurement of pressure and temperature in a supersonic ejector using FBG sensors](#)
Gautam Hegde, Balaji Himakar, Srisha Rao M V et al.
- [Calibration and modelling of ejector dilutors for automotive exhaust sampling](#)
Barouch Giechaskiel, Leonidas Ntziachristos and Zissis Samaras



ECS
The
Electrochemical
Society
Advancing solid state &
electrochemical science & technology

DISCOVER
how sustainability
intersects with
electrochemistry & solid
state science research

Simulation of ejector for vacuum generation

L Macia¹, R Castilla¹ and P J Gámez¹

¹Universitat Politecnica de Catalunya, Faculty of Fluid Mechanics, Carrer Colom 11 08222 Terrassa, Catalunya, Spain

E-mail: llorenc.macia@upc.edu, robert.castilla@upc.edu, pedro.javier.gomez@upc.edu

Abstract. Supersonic ejectors are used in a wide range of applications such as compression of refrigerants in cooling systems, pumping of volatile fluids, or vacuum generation. The objective of the present paper is to mesh and simulate, in an OpenFOAM environment with an open access implicit density- based solver HiSA, the physics of the vacuum ejector, and, later, compare the results with experimental measurements. In order to achieve this a 2D axisymmetric mesh made by hexahedral cells has been created. Steady solutions have been obtained, with prescribed total pressure in primary and secondary inlets. Secondary total pressure ranges from 1 to around 0.2 bar in which the secondary flow is zero. Numerical results are compared with experimental measurement, with two flowmeter sizes for small flow rate accuracy. Two regimes are encountered. In supercritical regime the secondary is choked and sonic flow is reached in the second nozzle. In subcritical regime, the secondary flow is subsonic. The agreement is good, although simulation tends to slightly overestimate flow rate for large values region.

1. Introduction

Supersonic ejectors are used in a wide range of applications such as compression of refrigerants in cooling systems, pumping of volatile fluids, or vacuum generation. In this latter case, also known as zero-secondary flow, physics in the vacuum ejector is more complicated than in steady cases, since recirculation bubbles existing in the diffuser exhibit transient behaviour during the start-up period [1].

In the supersonic ejectors the main concern is to achieve the maximum vacuum level and to increase the flow rate of suction. The induced flow, or secondary flow, is the air that is being carried across the second nozzle.

In Figure 1 a scheme of the primary and secondary flow, as well as the mixing chamber where both flows join, is presented. Figure 2 shows the model of the ejector simulated.

The purpose of the present paper is to numerically simulate an ejector and compare results with experimental measurements.



with low values of this pressure. Figure 4 shows a theoretical characteristic curve with a decreasing flow rate while increase the vacuum level.

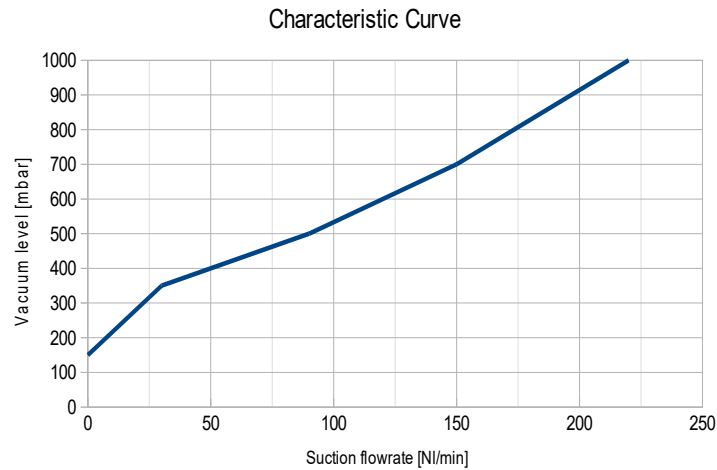


Figure 4. Standard curve of performance.

3. Numerical results

For a supersonic compressible flow, density based models are the favourite because of its capacity of capture discontinuities created by the shock waves. The equations for unsteady compressible flow are, for mass, momentum and energy,

$$\frac{\partial \rho}{\partial t} + \frac{\partial}{\partial x_i} \rho u_i = 0 \quad (1)$$

$$\frac{\partial}{\partial t} \rho u_i + \frac{\partial}{\partial x_j} \rho u_i u_j = -\frac{\partial p}{\partial x_i} + \mu \left(\frac{\partial u_i}{\partial x_j} + \frac{\partial u_j}{\partial x_i} - \frac{2}{3} \frac{\partial u_k}{\partial x_k} \delta_{ij} \right) \quad (2)$$

$$\frac{\partial}{\partial t} \rho E + \frac{\partial}{\partial x_j} \rho E u_j = -\frac{\partial u_i p}{\partial x_i} + \mu u_i \left(\frac{\partial u_i}{\partial x_j} + \frac{\partial u_j}{\partial x_i} - \frac{2}{3} \frac{\partial u_k}{\partial x_k} \delta_{ij} \right) + k \frac{\partial T}{\partial x_i} \quad (3)$$

with the perfect gases equation,

$$p = \rho R' T \quad (4)$$

have been solved on the OpenFOAM simulation toolbox. In the present paper the open access implicit density-based solver HiSA [4], that implements the AUSM+up upwind scheme for face fluxes, has been used. This solver allows to solve unsteady flows with larger Courant numbers than explicit solvers. According to Mazzelli [3], it has been proved that the best turbulence model are the k-w SST, and thus, it has been used in the present simulations.

The 2d axisymmetric hexahedra-dominated mesh has been generated with blockMesh, in order to get a suitable good quality. A python code that, eventually, creates the required dictionary, blockMeshDict, has been also used. This mesh is composed of 20300 cells. Figure 5 and Figure 6 show the total view of the mesh and the detail of the mixing chamber.

The boundary condition in primary inlet is 6 bar (relative) of total pressure, and Neumann condition for velocity. In the secondary inlet also the pressure is prescribed, and the flow rate is given by the simulation. In outlet the standard atmospheric pressure is set but, in order to avoid reflections, the waveTransmissive boundary condition is used.

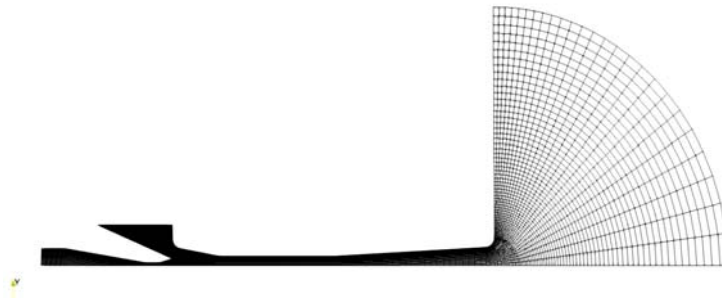


Figure 5. The mesh created by blockMesh.

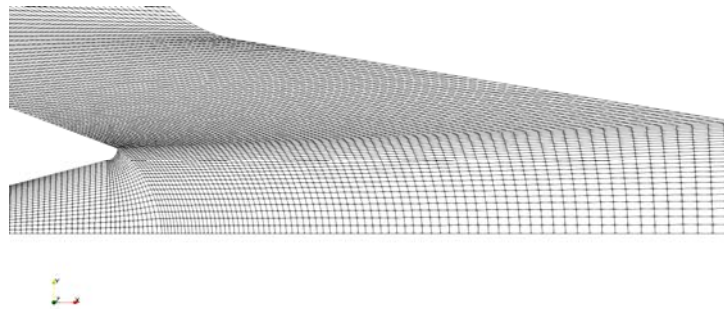


Figure 6. Detail of the critical part of the mesh.

A series of simulations, where the pressure at the secondary inlet has been changed, have been performed. The secondary pressure has ranged from atmospheric pressure (1 bar) to 0.2 bar. For each of this pressures the flow rate has been calculated.

4. Discussion

4.1. Experimental and numerical data

Figure 7 shows the numerical and the experimental results for the same geometry and operating conditions. A good agreement is found, although it seems that the numerical simulations overestimate the flow rate, about 10%, at the same vacuum pressure for small vacuum level of $P_s = 0.28$ up to $P_s = 1$ (large values of pressure in vacuum level) while underestimate the flow rate, about less than 5%, in the low values of vacuum pressure, at $P_s = 0.21$ up to $P_s = 0.28$.

It also tends to slightly overestimate the value of maximum pressure level: zero flow performance at $P_s = 0.2$ in the experimental results whereas $P_s = 0.217$ in the numerical ones.

4.2. Subcritical and critical modes

According to the thesis of Del Valle [2], it should be possible to observe a two regimens of secondary flow rate. So, at the beginning this flow is shocked at the very exit of the second nozzle. When at the vessel is at some vacuum level, the flow rate becomes sub-critical, and, finally, gets stuck so it becomes a zero-secondary flow ejector. In the fig, 8 is possible to see how the secondary flow is retained before the mixing chamber, due to the flow expansion of the primary flow.

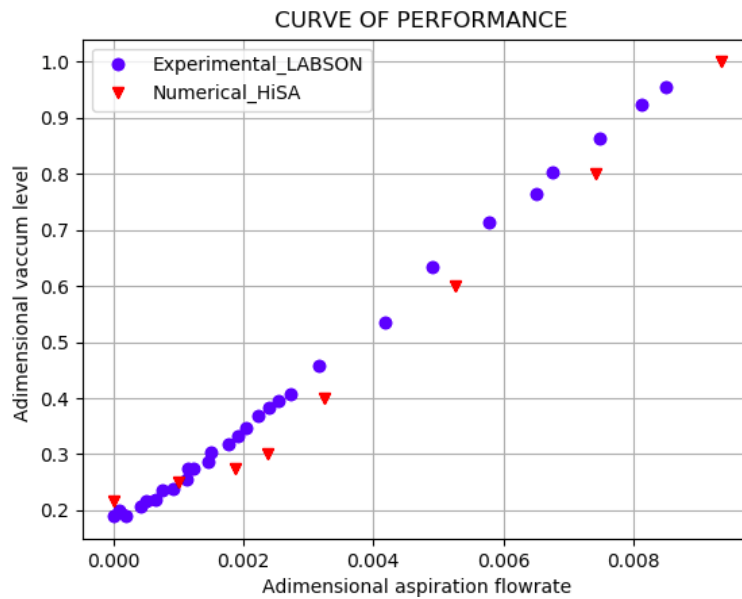


Figure 7. Curve of performance Experimental vs Numerical.

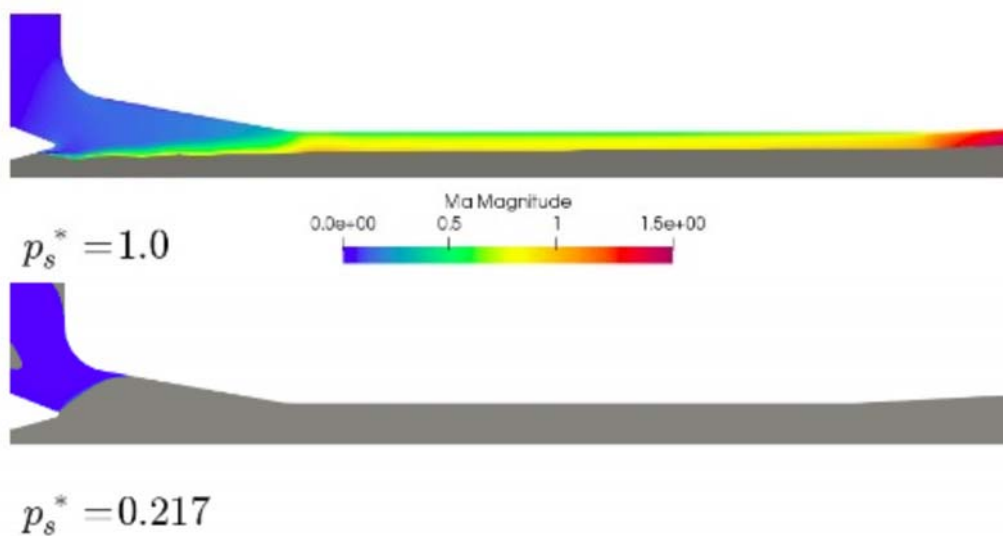


Figure 8. At 1.0 bar in the secondary field works in critical mode to work as zero-secondary flow at 0.217 bar.

5. Conclusion

Simulations of a supersonic ejector for vacuum generation have been presented. Simulations have been performed with the open source implicit density-based HiSA in the frame of the OpenFoam toolbox. Numerical results have been compared with experimental measurements, with an acceptable agreement, although CFD tend to slightly overestimate flow rate for the high values range.

It has been proved that the HiSA is a suitable implicit compressible gas based on density solver, and that it has been able to obtain results in less time expected than the explicit solvers.

The ejector simulated goes from a critical mode to a zero-secondary flow at 0,217 bar, which is approximately 80% of vacuum level.

Acknowledgments

Support of Industrial Doctorate (2018 DI 025) from Generalitat de Catalunya is acknowledged. Many thanks to laboratory technicians Jaume Bonastre, father and son, for their help. Special thanks to Oliver Oxtoby, from CSIR (South Africa) for his invaluable comments.

References

- [1] Jafarian A, Azizi M, and Forghani P 2016 Experimental and numerical investigation of transient phenomena in vacuum ejectors, *Energy* **102** 528–536
- [2] García V 2014 *Eyectores para aplicaciones frigoríficas*, PhD thesis, Valladolid
- [3] Mazzelli F, Little A B, Garimella S, and Bartosiewicz Y 2015 Computational and experimental analysis of supersonic air ejector: Turbulence modeling and assessment of 3D effects *Int. J. Heat Fluid Flow*, **56** 305–316
- [4] Snedde G, Heyns J and Oxtoby O 2018 *HISA*, <https://hisa.gitlab.io> (accessed on Jan, 2019)
- [5] Gao X 2018 Developing a parallel density-based implicit solver with mesh deformation in OpenFOAM, *J. Comput. Sci.* **28** 59–69
- [6] Kumar R A and Rajesh G 2018 Physics of vacuum generation in zero-secondary flow ejectors, *Phys. Fluids* **30** 100-121